28

Impact of Mass Transfer on Modelling and Simulation of Reactive Distillation Columns

Zuzana Švandová, Jozef Markoš and Ľudovít Jelemenský
Institute of Chemical and Environmental Engineering, Slovak University of Technology, Radlinského 9, 812 37, Bratislava, Slovakia

1. Introduction

1.1 Reactive distillation

In chemical process industries, chemical reaction and purification of the desired products by distillation are usually carried out sequentially. In many cases, the performance of this classic chemical process structure can be significantly improved by an integration of reaction and distillation in a single multifunctional process unit. This integration concept is called 'reactive distillation' (RD); when heterogeneous catalysts are applied, the term 'catalytic distillation' is often used. As to the advantages of this integration, chemical equilibrium limitations can be overcome, higher selectivity achieved, by-product formation reduced, heat of the reaction can be used for distillation in-situ, hot spots and run-away effect can be avoided, and azeotropic or closely boiling mixtures can be separated more easily than in a non-RD process. Some of these advantages are realised using a reaction to improve the separation; others are realised using separation to improve the reaction (Sundmacher & Kienle, 2002). Technological advantages as well as financial benefit resulting from this integration are important. Simplification or elimination of the separation system can lead to significant capital savings, increased conversion and total efficiency, which then result in reduced operating costs (Taylor & Krishna, 2000).

1.2 Complexity of RD

The design and operation issue of RD systems are considerably more complex than those involved in either conventional reactors or conventional distillation columns. The introduction of an in-situ separation function within the reaction zone leads to complex interactions between the vapour-liquid equilibrium, vapour-liquid mass transfer, intra-catalyst diffusion (for heterogeneously catalysed processes), chemical kinetics and equilibrium. Such interactions, along with strong nonlinearities introduced by coupling of diffusion and chemical kinetics of counter-current contacting, have been proved to lead to the phenomenon of multiple steady states and complex dynamics, which has been verified in experimental laboratory and pilot plant units (Taylor & Krishna, 2000). Mathematical model of reactive distillation consists of sub-models for mass transfer, reaction and hydrodynamics whose complexity and rigour vary within a broad range (Taylor & Krishna, 2000; Noeres et al., 2003). For example, mass transfer between the gas/vapour and the liquid phase can be described on basis of the most rigorous rate-based approach, using the

Maxwell-Stefan diffusion equations, or it can be accounted for by a simple equilibrium stage model assuming thermodynamic equilibrium between both phases. Homogeneously catalysed reactive distillation, with a liquid catalyst acting as a mixture component, and auto-catalysed reactive distillation present essentially a combination of transport phenomena and reactions taking place in a liquid film (Sláva et al., 2008; Sláva et al., 2009). With heterogeneous systems, it is generally necessary to consider also the particular processes around and inside the solid catalyst particle (Kotora et al., 2009). Modelling of hydrodynamics in multiphase gas/vapour - liquid contactors includes an appropriate description of axial dispersion, liquid hold-up and pressure drop. The correlations providing such descriptions have been published in numerous papers and are collected in several reviews and textbooks. The most suitable approach to reactive distillation modelling depends not only on the model quality and program convergence but also on the quality of model parameters. It is obvious that the choice of the right modelling approach must be harmonised with the availability of the model parameters necessary for the selected model. Optimal complexity of the model for reactive separations depends on one hand on the model accuracy but on the other hand also on the availability of model parameters and the efficiency of simulation methods (Górak, 2006). In this chapter, we focused our attention on vapour-liquid mass transfer influence on the prediction of RD column behaviour neglecting the liquid-solid and intraparticle mass transfer. It means that the bulk phase with solid catalyst was assumed to be homogeneous.

1.3 Mathematical models of a reactive distillation column

Complex behaviour caused by the vapour-liquid interaction, heat effects, thermodynamic and hydrodynamic regimes called for the necessity of models able to describe all these interactions. Starting with the well know McCabe-Thiele graphical method for binary distillation, the approximate shortcut method for multicomponent mixtures according to the Smith-Brinkley or the Fenske-Underwood-Gilliland method, equation tearing procedures using the tridiagonal matrix algorithm or the inside-out method, etc. (Perry et al., 1997) have been used in the history of distillation and reactive distillation modelling. But only with the starting development of computer art, could the researchers start to use standard practices used in chemical engineering calculations without any restrictions in respect to the equations complexity. At the present time, different depth approaches such as the equilibrium (EQ) stage model, EQ stage model with stage efficiencies, nonequilibrium (NEQ) stage model, NEQ cell model and the CFD model can be found in literature on RD column design. Simultaneously, there are several possible versions of the NEQ model formulations with reference to the description of the vapour-liquid equilibrium, reaction equilibrium and kinetics (homogenous/heterogeneous reaction, pseudo-homogenous approach), mass transfer (effective diffusivity method, Maxwell-Stefan approach) and hydrodynamics (completely mixed vapour and liquid, plug-flow vapour, eddy diffusion model for the liquid phase, etc.).

1.3.1 Equilibrium stage model

The main idea is in assuming that the vapour and liquid streams leaving an equilibrium stage are in complete equilibrium with each other and the thermodynamic relations can be used to determine the equilibrium stage temperature and relate the concentrations in the equilibrium streams at a given pressure (Perry et al., 1997). Schematic diagram of an equilibrium stage is shown in Fig. 1. Vapour from the stage below and liquid from the stage

above are brought into contact on the stage together with other fresh or recycled feeds. The vapour and liquid streams leaving the stage are assumed to be in equilibrium with each other.

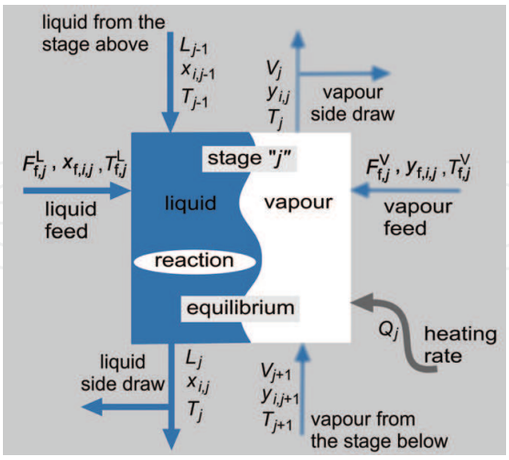

Fig. 1. Equilibrium stage

MESH equations of the equilibrium model for the *j*-th stage

- M equations are the material balance equations;

the total material balance

$$\mathbf{M}_j \equiv \frac{dU_j}{dt} = \sum_{f=1}^{N_F} F_{f,j} + \sum_{r=1}^{N_R}\left(\dot{\xi}_{r,j}\sum_{i=1}^{N_I}\nu_{r,i}\right) + L_{j-1} + V_{j+1} - \left(1+r_j^{\mathrm{V}}\right)V_j - \left(1+r_j^{\mathrm{L}}\right)L_j$$

material balance for component *i*

$$\mathbf{M}_{i,j} \equiv \frac{d\left(U_j x_{i,j}\right)}{dt} = \sum_{f=1}^{N_F} F_{f,j}x_{f,i,j} + \sum_{r=1}^{N_R}\left(\dot{\xi}_{r,j}\nu_{r,i}\right) + L_{j-1}x_{i,j-1} + V_{j+1}y_{i,j+1} - \left(1+r_j^{\mathrm{L}}\right)L_j x_{i,j}$$

$$-\left(1+r_j^{\mathrm{V}}\right)V_j y_{i,j}$$

- E equations are the phase equilibrium relations

$$\mathbf{E}_j \equiv K_{i,j}x_{i,j} - y_{i,j} = 0$$

- S equations are the summation equations in each phase

$$\mathbf{S}_j^{\mathrm{L}} \equiv 1 - \sum_{i=1}^{N_I} x_{i,j} = 0\,,\ \mathbf{S}_j^{\mathrm{V}} \equiv 1 - \sum_{i=1}^{N_I} y_{i,j} = 0$$

- Heat balance*

$$\mathbf{H}_j \equiv \frac{d(U_j H_j^{\mathrm{L}})}{dt} = \sum_{f=1}^{N_F} F_{f,j}H_{f,j} + \sum_{r=1}^{N_R}\dot{\xi}_{r,j}\left(-\Delta_r H_{r,j}\right) + L_{j-1}H_{j-1}^{\mathrm{L}} + V_{j+1}H_{j+1}^{\mathrm{V}}$$

$$-\left(1+r_j^{\mathrm{L}}\right)L_j H_j^{\mathrm{L}} - \left(1+r_j^{\mathrm{V}}\right)V_j H_j^{\mathrm{V}} + Q_j$$

- Initial conditions, for $t = 0$

$$x_{i,j} = x_{i,j}^0\,,\ y_{i,j} = y_{i,j}^0\,,\ T_j = T_j^0\,,\ V_j = V_j^0\,,\ L_j = L_j^0$$

* *reference state: pure component in the liquid phase at 273.15 K*

Table 1. Specific equations of the equilibrium stage model

A complete reactive distillation column is considered to be a sequence of such stages. Equations describing the equilibrium stages are known as **MESH** equations, **MESH** being an acronym referring to the different types of equations: **M**aterial balances, vapour–liquid **E**quilibrium equations, mole fraction **S**ummations and enthalpy (**H**) balances (Taylor & Krishna, 1993; Kooijman & Taylor, 2000; Taylor & Krishna, 2000). A summary of specific equations is given in Table 1.

1.3.2 Nonequilibrium stage model

An NEQ model for RD follows the philosophy of rate-based models for conventional distillation (Krishnamurthy & Taylor, 1985a; Krishnamurthy & Taylor, 1985b; Taylor & Krishna, 1993; Taylor et al., 1994; Kooijman & Taylor, 2000). In contrary to the EQ model, the NEQ model does not assume thermodynamic equilibrium on the whole stage, but only at the vapour-liquid interface. Mass transfer resistances are located in films near the vapour-liquid and liquid-solid (for heterogeneously catalysed processes) interfaces. The description of the interphase mass transfer, in either fluid phase, is almost invariably based on the film theory and rigorous Maxwell-Stefan theory for the interphase heat and mass transfer rates calculation. Schematic diagram of the nonequilibrium concept is shown in Fig. 2. Vapour and liquid feed streams are contacted on the stage and allowed to exchange mass and energy across their common interface represented in the diagram by a vertical wavy line. A complete reactive distillation column is considered a sequence of these stages. In a nonequilibrium model, separate balance equations are written for each phase on each stage. Conservation equations for each phase are linked by material balances around the interface.

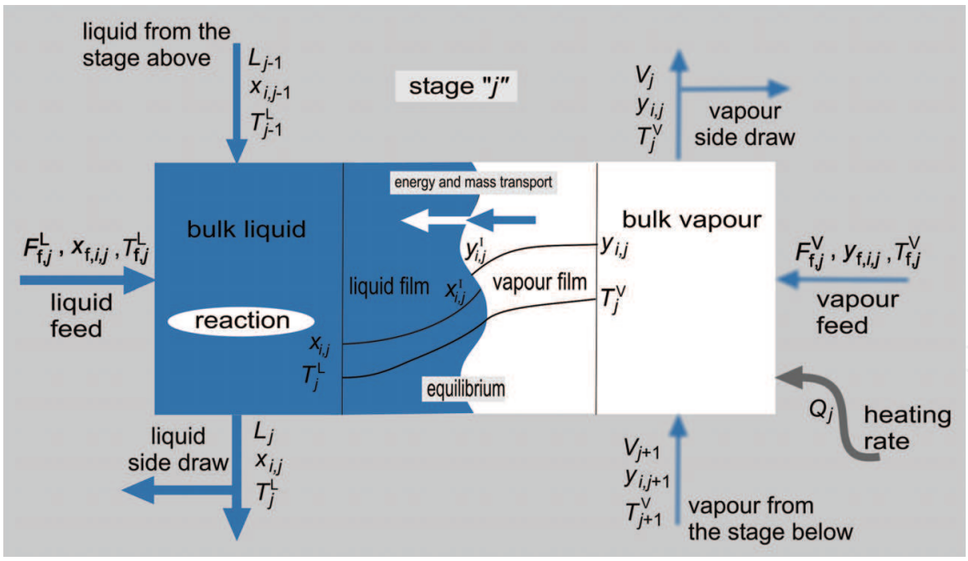

Fig. 2. Nonequilibrium stage

Equilibrium relations are used to relate the composition on each side of the phase interface. The interface composition and temperature must, therefore, be determined as a part of a nonequilibrium column simulation. Equations describing a nonequilibrium stage are **M**aterial balances, **E**nergy balances, **R**ate equations, **S**ummation equations, **H**ydraulic equation, and e**Q**uilibrium relations, i.e. **MERSHQ** equations. A summary of them is given in Table 2.

MERSHQ equations of the nonequilibrium model

- Total **(M)**aterial balances for each phase

$$\mathbf{M}_j^{\mathrm{V}} \equiv \frac{dU_j^{\mathrm{V}}}{dt} = \sum_{f=1}^{N_F^{\mathrm{V}}} F_{f,j}^{\mathrm{V}} + V_{j+1} - \left(1 + r_j^{\mathrm{V}}\right) V_j - \mathcal{N}_{t_j}^{\mathrm{V}}$$

$$\mathbf{M}_j^{\mathrm{L}} \equiv \frac{dU_j^{\mathrm{L}}}{dt} = \sum_{f=1}^{N_F^{\mathrm{L}}} F_{f,j}^{L} + \sum_{r=1}^{N_R} \left(\dot{\xi}_{r,j} \sum_{i=1}^{N_I} \nu_{r,i} \right) + L_{j-1} - (1 + r_j^{\mathrm{L}}) L_j + \mathcal{N}_{t_j}^{\mathrm{L}}$$

material balances for component *i* for each phase

$$\mathbf{M}_{i,j}^{\mathrm{V}} \equiv \frac{d\left(U_j^{\mathrm{V}} y_{i,j}\right)}{dt} = \sum_{f=1}^{N_F^{\mathrm{V}}} F_{f,j}^{\mathrm{V}} y_{f,i,j} + V_{j+1} y_{i,j+1} - (1 - r_j^{\mathrm{V}}) V_j y_{i,j} - \mathcal{N}_{i,j}^{\mathrm{V}}$$

$$\mathbf{M}_{i,j}^{\mathrm{L}} \equiv \frac{d\left(U_j^{\mathrm{L}} x_{i,j}\right)}{dt} = \sum_{f=1}^{N_F^{\mathrm{L}}} F_{f,j}^{\mathrm{L}} x_{f,i,j} + \sum_{r=1}^{N_R} \left(\dot{\xi}_{r,j} \nu_{r,i} \right) + L_{j-1} x_{i,j-1} - (1 + r_j^{\mathrm{L}}) L_j x_{i,j} + \mathcal{N}_{i,j}^{\mathrm{L}}$$

- **(E)**nergy balance equations for each phase*

$$\mathbf{E}_j^{\mathrm{V}} \equiv \frac{d(U_j^{\mathrm{V}} H_j^{\mathrm{V}})}{dt} = \sum_{f=1}^{N_F^{\mathrm{V}}} F_{f,j}^{\mathrm{V}} H_{f,j}^{\mathrm{V}} + V_{j+1} H_{j+1}^{\mathrm{V}} - \left(1 + r_j^{\mathrm{V}}\right) V_j H_j^{\mathrm{V}} + Q_j^{\mathrm{V}} - \mathcal{E}^{\mathrm{V}}$$

$$\mathbf{E}_j^{\mathrm{L}} \equiv \frac{d(U_j^{\mathrm{L}} H_j^{\mathrm{L}})}{dt} = \sum_{f=1}^{N_F^{\mathrm{L}}} F_{f,j}^{\mathrm{L}} H_{f,j}^{\mathrm{L}} + \sum_{r=1}^{N_R} \dot{\xi}_{r,j} \left(-\Delta_r H_{r,j}\right) + L_{j-1} H_{j-1}^{\mathrm{L}}$$

$$-\left(1 + r_j^{\mathrm{L}}\right) L_j H_j^{\mathrm{L}} + Q_j^{\mathrm{L}} + \mathcal{E}^{\mathrm{L}}$$

(E)nergy balance around the interface: $\mathbf{E}_j^{I} \equiv \mathcal{E}_j^{\mathrm{V}} - \mathcal{E}_j^{\mathrm{L}} = 0$

- **(R)**ate equations: $\mathcal{N}_{i,j} - \mathcal{N}_{i,j}^{\mathrm{L}} = 0$, $\mathcal{N}_{i,j} - \mathcal{N}_{i,j}^{V} = 0$
- Mole fractions must **(S)**um to unity in each phase:

Bulk liquid: $\mathbf{S}_j^{\mathrm{L}} \equiv \sum_{i=1}^{N_I} x_{i,j} - 1 = 0$ bulk vapour: $\mathbf{S}_j^{\mathrm{V}} \equiv \sum_{i=1}^{N_I} y_{i,j} - 1 = 0$

liquid film: $\mathbf{S}_j^{\mathrm{LI}} \equiv \sum_{i=1}^{N_I} x_{i,j}^{\mathrm{I}} - 1 = 0$ vapour film: $\mathbf{S}_j^{\mathrm{VI}} \equiv \sum_{i=1}^{N_I} y_{i,j}^{\mathrm{I}} - 1 = 0$

(H)ydraulic equations: $\mathbf{H}_j \equiv P_j - P_{j-1} - (\Delta P_{j-1}) = 0$

- Phase e**(Q)**uilibrium is assumed to exist only at the interface: $\mathbf{Q}_{i,j}^{\mathrm{I}} \equiv K_{i,j} x_{i,j}^{\mathrm{I}} - y_{i,j}^{\mathrm{I}} = 0$
- **Initial conditions**, for $t = 0$: $x_{i,j} = x_{i,j}^0$, $y_{i,j} = y_{i,j}^0$, $x_{i,j}^{\mathrm{I}} = \left(x_{i,j}^{\mathrm{I}}\right)^0$, $y_{i,j}^{\mathrm{I}} = \left(y_{i,j}^{\mathrm{I}}\right)^0$,

$V_j = V_j^0$, $L_j = L_j^0$, $T_j^L = \left(T_j^L\right)^0$, $T_j^V = \left(T_j^V\right)^0$, $T_j^{\mathrm{I}} = \left(T_j^{\mathrm{I}}\right)^0$, $\mathcal{N}_{i,j} = \mathcal{N}_{i,j}^0$, $P_j = \left(P_j\right)^0$

** reference state: pure component in the liquid phase at 273.15 K*

Table 2. Specific equations of the nonequilibrium stage model

Building an NEQ model of reactive separation is not as straightforward as it is with the EQ stage model in which a term accounting for a reaction is added to the liquid-phase material balances (Taylor & Krishna, 2000). A nonequilibrium simulation needs more detailed specifications (in comparison with an equilibrium model). For illustration, we need to know whether the reaction is heterogeneous or homogeneous, also the type and layout of the column internals, mass transfer coefficient model, flow model for both phases, pressure drop model, physical properties models, etc., are important. For the estimation of mass and heat transport properties, the nonequilibrium model requires an evaluation of many more physical properties, such as viscosities, diffusivities, thermal conductivities, surface tension, which are not needed in an equilibrium model. In order to determine the mass transfer coefficients, interfacial area and pressure drop, column type and internals layout must be known.

1.3.2.1 Mass and heat transfer in NEQ model

For the mass transfer on a stage, the well known two-film model which assumes that, for each phase, the transport resistance is concentrated in a thin film adjacent to the phase interface is often adopted. The thickness of these hypothetical films is in the range of 0.001-0.1 mm for the liquid phase and in the range of 0.1-1 mm for the gas phase (Taylor & Krishna, 1993). The most fundamentally sound way to model mass transfer in multicomponent systems is to use the Maxwell-Stefan theory (see Taylor & Krishna (1993) Krishna & Wesselingh (1997)). Another approach to modelling mass transfer in multicomponent systems is enabled by the Fick's law (Sláva et al., 2008; Kotora et al., 2009). Complexity of the Maxwell-Stefan equations and the generalised Fick's law have led to the use of simpler constitutive relations, e.g. effective diffusivity. Extensive and detailed description of multicomponent mass transfer was provided by Taylor & Krishna (1993). The nonequilibrium model uses two sets of mass transfer **(R)**ate equations (see Table 2). At the V-L interface, there is continuity of molar rates:

$$\mathcal{N}_{i,j}^{V} - \mathcal{N}_{i,j}^{L} = 0 \tag{1}$$

Molar rates in each phase are computed from diffusive and convective contributions (Kooijman & Taylor, 2000; Taylor & Krishna, 2000):

$$\mathcal{N}_{i,j}^{L} = a_j^{\mathrm{I}} J_{i,j}^{\mathrm{L}} + x_{i,j} \mathcal{N}_{\mathrm{t},j}^{L} \tag{2}$$

$$\mathcal{N}_{i,j}^{V} = a_j^{\mathrm{I}} J_{i,j}^{V} + y_{i,j} \mathcal{N}_{\mathrm{t},j}^{V} \tag{3}$$

Molar diffusion fluxes $J_{i,j}^{\mathrm{L}}$ and $J_{i,j}^{V}$ (in the matrix form) are given as follows:

$$\left(J_j^{\mathrm{L}}\right) = c_{\mathrm{t},j}^{\mathrm{L}} \left[k_j^{\mathrm{L}}\right] \left(x_j^{\mathrm{I}} - x_j\right) \tag{4}$$

$$\left(J_j^{\mathrm{V}}\right) = c_{\mathrm{t},j}^{\mathrm{V}} \left[k_j^{\mathrm{V}}\right] \left(y_j - y_j^{\mathrm{I}}\right) \tag{5}$$

Note that there are only (N_{I}-1) × (N_{I}-1) elements in the [k_{j}] matrices (Taylor & Krishna, 1993). Matrices of multicomponent mass transfer coefficients assuming ideal behaviour of the vapour phase can be calculated from:

$$\left[k_j^V\right] = \left[R^{\mathrm{V}}\right]^{-1} \tag{6}$$

$$\left[k_j^L\right] = \left[R^L\right]^{-1}\left[\Gamma\right] \tag{7}$$

where [Γ] is the matrix of thermodynamic correction factors portraying nonideal behaviour of the liquid phase and [R^P] is the matrix of mass transfer resistances for phase P calculated from:

$$R_{i,i}^P = \frac{z_i^P}{\kappa_{i,N_t}^P} + \sum_{\substack{k=1 \\ k\neq i}}^{N_t} \frac{z_k^P}{\kappa_{i,k}^P} \tag{8}$$

$$R_{i,j(i\neq j)}^P = -z_i^P\left(\frac{1}{\kappa_{i,j}^P} - \frac{1}{\kappa_{i,N_t}^P}\right) \tag{9}$$

where z^P is the mole fraction for phase P and $\kappa_{i,j}^P$ is the mass transfer coefficient for the binary *i-j* pair in phase *P*.

A necessary complementary equation is the **(E)**nergy balance for the interface. It presents the continuity of the energy fluxes across the V-L interface (Table 2). Heat transfer rates for the two phases, $\mathcal{E}_j^{\mathrm{V}}$, $\mathcal{E}_j^L$ are defined as:

$$\mathcal{E}_j^L = h_j^{\mathrm{L}} a_j^{\mathrm{I}}\left(T_j^{\mathrm{I}} - T_j^{\mathrm{L}}\right) + \sum_{i=1}^{N_t} \mathcal{N}_{i,j} H_{i,j}^{\mathrm{L}} \tag{10}$$

$$\mathcal{E}_j^{\mathrm{V}} = h_j^{\mathrm{V}} a_j^{\mathrm{I}} \frac{\varepsilon_j^{\mathrm{V}}}{\exp \varepsilon_j^{\mathrm{V}} - 1}\left(T_j^{\mathrm{V}} - T_j^{\mathrm{I}}\right) + \sum_{i=1}^{N_t} \mathcal{N}_{i,j} H_{i,j}^{\mathrm{V}} \tag{11}$$

where h_j^{L} and h_j^V are the liquid and the vapour heat transfer coefficients, $H_{i,j}^{\mathrm{L}}$ and $H_{i,j}^{\mathrm{V}}$ are the liquid and the vapour partial molar enthalpies of component *i*, and $\varepsilon_j^{\mathrm{V}}$ is the heat transfer rate factor (Krishnamurthy & Taylor, 1985b) defined as:

$$\varepsilon_j^{\mathrm{V}} = \sum_{i=1}^{N_t} \mathcal{N}_{i,j} C_{pi,j}^{\mathrm{V}} / \left(h_j^{\mathrm{V}} a_j^{\mathrm{I}}\right) \tag{12}$$

To calculate the vapour phase heat transfer coefficients, the Chilton-Colburn analogy between mass and heat transfer may be used (Krishnamurthy & Taylor, 1985b; Kooijman & Taylor, 2000):

$$h_j^{\mathrm{V}} = c_{\mathrm{t},j}^{\mathrm{V}} \kappa_{\mathrm{av},j}^{\mathrm{V}} C_{pm,j}^{\mathrm{V}} \left(Le_j^{\mathrm{V}}\right)^{2/3} \tag{13}$$

For the calculation of the liquid phase heat transfer coefficients, a penetration model may be used (Kooijman & Taylor, 2000):

$$h_j^{\mathrm{L}} = c_{\mathrm{t},j}^{\mathrm{L}} \kappa_{\mathrm{av},j}^{\mathrm{L}} C_{pm,j}^{\mathrm{L}} \left(Le_j^{\mathrm{L}} \right)^{1/2} \tag{14}$$

where $\kappa_{\mathrm{av},j}^{\mathrm{L}}$ and $\kappa_{\mathrm{av},j}^{V}$ are the average values of binary mass transfer coefficients for each phase, Le_j^{L} and Le_j^{V} are the Lewis numbers for each phase, $C_{p\mathrm{m},j}^{V}$ and $C_{p\mathrm{m},j}^{\mathrm{L}}$ are the heat capacities of vapour and liquid mixtures.

Bubble-Cap tray	Sieve tray	Valve tray	Dumped packing	Structured packing
AICHE (1958) Hughmark (1971)	AICHE (1958) Chan-Fair (1984) Zuiderweg (1982) Chen-Chuang (1993) Harris (1965) Bubble-Jet	AICHE (1958)	Onda-Takeuchi-Okumoto (1968) Bravo-Fair (1982) Biller-Schultes (1992) …	Bravo-Rocha-Fair (1985) Bravo-Rocha-Fair (1992) Billet-Schultes (1992) …

Table 3. Available mass transfer coefficient correlations per internal type suggested by (Kooijman & Taylor, 2000)

Crucial parameters in a nonequilibrium model are the mass transfer coefficients. The choice of mass transfer coefficient correlations can influence the results of a simulation (Kooijman & Taylor, 2000). In Eqs. (8), (9), (13) and (14), the flux mass transfer coefficients (κ) were used which may be estimated using empirical correlations with the Maxwell-Stefan diffusivity of the appropriate *i-j* pair ($Đ_{i,j}$) replacing the binary Fick's diffusivity ($D_{i,j}$) (Taylor & Krishna, 1993). Table 3 provides a summary of the available mass transfer coefficient correlations for tray and packed columns suggested by Kooijman & Taylor (2000). The binary mass transfer coefficients obtained from these correlations are functions of the tray design and layout, or of the packing type and size, as well as of the operational parameters and physical properties including the binary pair diffusion coefficients. Table 4 introduces four chosen empirical correlations for the estimation of the number of transfer units or relations for the estimation of binary mass transfer coefficients for a sieve tray. Binary mass transfer coefficients can be computed from the number of transfer units (**N**) (Taylor & Krishna, 1993; Kooijman & Taylor, 2000) as follows:

$$\mathbf{N}^{\mathrm{V}} = k^{\mathrm{V}} a^{\mathrm{V}} t^{\mathrm{V}} = k^{\mathrm{V}} a h_f / u_s \tag{15}$$

$$\mathbf{N}^{\mathrm{L}} = k^{\mathrm{L}} a^{L} t^{\mathrm{L}} = k^{\mathrm{L}} a h_f Z / \left(Q^{\mathrm{L}} / W \right) \tag{16}$$

where Z is the liquid flow path length (m), W is the weir length (m), Q^{L} is the volumetric liquid flow rate ($m^3\ s^{-1}$), h_f is the froth height (m), a^{V} and a^{L} are the interfacial area per unit volume of vapour and liquid ($m^2\ m^{-3}$), respectively, a is the interfacial area per unit volume of froth ($m^2\ m^{-3}$). Parameter ah_f ($m^2\ m^{-2}$) can be estimated from the Zuiderweg's (1982) method (see Table 4), where it is dependent on the regime of operation (spray regime or mixed froth-emulsion flow regime), and u_s is the superficial vapour velocity ($m\ s^{-1}$) based on the bubbling area of the tray, A_b:

$$u_s = \frac{Q^{\mathrm{V}}}{A_b} = \frac{V}{c_t^{\mathrm{V}} A_b} \tag{17}$$

where Q^{V} is the volumetric vapour flow rate ($m^3\ s^{-1}$), V is the vapour flow rate (mol s^{-1}) and c_t^{V} is the molar concentration of the vapour mixture (mol m^{-3}).

Method	*Other relations*	*Number of transfer units (**N**) [-]*
AICHE (1958)	$F_s = u_s \left(\rho_t^{\mathrm{V}}\right)^{0.5}$ $Sc^{\mathrm{V}} = \mu^{\mathrm{V}} / \left(\rho_t^{\mathrm{V}} D^{\mathrm{V}}\right)$ $t^{\mathrm{L}} = h_L Z W / Q^{\mathrm{L}}$	$\mathbf{N}^{\mathrm{L}} = 19700\left(D^{\mathrm{L}}\right)^{0.5}\left(0.4F_s + 0.17\right)t^{\mathrm{L}}$ $\mathbf{N}^{\mathrm{V}} = \left(0.776 + 4.57h_w - 0.238F_s + \frac{104.8Q^{\mathrm{L}}}{W}\right)\sqrt{Sc^{\mathrm{V}}}$
Chan-Fair (1984)	$t^{\mathrm{V}} = \left(1-\alpha_e\right)h_L / \left(\alpha_e u_s\right)$ $F_f = u_s / u_{sf}$	$\mathbf{N}^{\mathrm{V}} = \left(103000 - 8670F_f\right)F_f\left(D^{\mathrm{V}}\right)^{0.5} t^{\mathrm{V}} h_L^{-0.5}$ $\mathbf{N}^{\mathrm{L}}$ – the AICHE correlation can be used
Chen-Chuang (1993)	$t^{\mathrm{V}} = h_L / u_s$ $F_s = u_s \left(\rho_{\mathrm{t}}^{\mathrm{V}}\right)^{0.5}$ $t^{\mathrm{L}} = t^{\mathrm{V}}\rho_{\mathrm{t}}^{\mathrm{L}} / \rho_{\mathrm{t}}^{\mathrm{V}}$ $\beta = A_h / A_b$	$\mathbf{N}^{\mathrm{V}} = 11\frac{1}{\left(\mu^{\mathrm{L}}\right)^{0.1}\beta^{0.14}}\left(\frac{\rho_{\mathrm{t}}^{\mathrm{L}}F_s^2}{\sigma^2}\right)^{1/3}\sqrt{D^{\mathrm{V}}t^{\mathrm{V}}}$ $\mathbf{N}^{\mathrm{L}} = 14\frac{1}{\left(\mu^{\mathrm{L}}\right)^{0.1}\beta^{0.14}}\left(\frac{\rho_{\mathrm{t}}^{\mathrm{L}}F_s^2}{\sigma^2}\right)^{1/3}\left(\frac{M^{\mathrm{V}}V}{M^{\mathrm{L}}L}\right)\sqrt{D^{\mathrm{L}}t^{\mathrm{L}}}$
		Mass transfer coefficients (k) [m s^{-1}]
Zuiderweg (1982)		$k^{\mathrm{V}} = 0.13 / \rho_{\mathrm{t}}^{\mathrm{V}} - 0.065 / \left(\rho_{\mathrm{t}}^{\mathrm{V}}\right)^2 \quad (1 < \rho_{\mathrm{t}}^{\mathrm{V}} < 80\ \mathrm{kg/m^3})$ $k^{\mathrm{L}} = 0.26\times10^{-5}\left(\mu^{\mathrm{L}}\right)^{-0.25}$ or $k^{\mathrm{L}} = 0.024\left(D^{\mathrm{L}}\right)^{0.25}$
	Other relations	*Interfacial area per unit bubbling area (ah_f) [$m^2\ m^{-2}$]*
Zuiderweg (1982)	$\mathrm{FP} = \frac{M^{\mathrm{L}}}{M^{\mathrm{V}}}\left(\frac{\rho_{\mathrm{t}}^{\mathrm{V}}}{\rho_{\mathrm{t}}^{\mathrm{L}}}\right)^{0.5}$ $b = W / A_b$ $h_L = 0.6h_w^{0.5}\left(\frac{p\mathrm{FP}}{b}\right)^{0.25}$ $\beta = A_h / A_b$	if FP > $3.0bh_L$ then froth-emulsion regime *Spray regime*: $ah_f = \frac{40}{\beta^{0.3}}\left(\frac{u_s^2\rho_{\mathrm{t}}^{\mathrm{V}}h_L FP}{\sigma}\right)^{0.37}$ *Froth-emulsion regime*: $ah_f = \frac{43}{\beta^{0.3}}\left(\frac{u_s^2\rho_{\mathrm{t}}^{\mathrm{V}}h_L FP}{\sigma}\right)^{0.53}$

Table 4. Empirical correlation for estimation of the number of transfer units, binary mass transfer coefficients and interfacial area per unit bubbling area

2. Utilisation of mathematical modelling

Mathematical modelling endeavours to provide a true projection of equipment behaviour not only for existing plants but also for designed technologies and equipments when

experimental data are insufficient. Steady state modelling provides information about selectivity, conversion, and production in dependence on the column (reactor) configuration and operational mode. Moreover, it gives information about physical properties of the output streams, temperature and concentration profiles in the entire column. This information is needed for the design and optimisation of the process. In the process design phase, dynamic simulation is needed to determine dynamic response to process disturbances. Using dynamic simulations, the start-up and shut-down of current processes can also be optimised. In recent years, mathematical modelling has often been used for the purposes of safety analysis (Molnár et al., 2005).

European direction 96/82/EC on control of major industrial accidents (so called Seveso II) requires a detailed safety analysis not only for existing industrial units, but also for units (technologies, equipments) which are designed. A useful tool for such an analysis is mathematical modelling of equipment linked with a methodology used for safety analysis, like HAZOP or others (Checklists method, What if? Analysis, FMECA (Failure Mode, Effect and Criticality Analysis)). A safety analysis includes an analysis of the multiplicity of steady states and their stability, identification of states leading to hazardous reactor behaviour, i.e. crossing of the practical stability limit, study of safe operating conditions, investigation of conditions and trajectories which can shift the reactor/column from one steady state to another one and the determination of a safe start-up and shut down procedure. Mohl et al. (1999) showed that the multiplicity found for a reactive distillation column has the same cause as that found for a continuous stirred tank reactor (CSTR). The existence of multiple steady states can result in both technological problems and dangerous situations. However, consequences of undesirable situations for a CSTR (other type of reactors) and a reactive distillation column may be completely different. For example, increased production of heat in a CSTR can result in the run-away effect, but in a reactive distillation column, the heat of reaction is used in-situ for evaporation and can (but does not have to) cause technological problems.

HAZOP is one of the best and most rigorous techniques for the identification of hazard and operability problems in a chemical plant (Kletz, 1999). The HAZOP procedure formally examines all equipment step by step as well as deviations from its normal operation conditions and considers what failures can occur. The HAZOP report includes all deviations, their causes, consequences in the equipment performance, analysis of these consequences, implemented protection (active and/or passive), and the resulting suggestions. It can be successfully applied not only for existing plants but also for designed technologies and equipment. On the other hand, two essential drawbacks of the HAZOP study exist. The primary drawback of the HAZOP approach is related to the possibility that hazards and operability problems may be overlooked. HAZOP requires many hours of work of a team of experienced engineers, and it is not easy to record the engineering reasoning, basic input information or the results. Therefore is the application of the HAZOP technique to a detailed chemical plant design a complex and time consuming task. Both these drawbacks can be reduced by integrating a model approach into HAZOP. Usually does the HAZOP analysis not consider the duration and amplitude of the deviations generated during the reactor operation. However, what does the deviation 'less flow' exactly mean; 90 % or 20 % of the usual operational value? Does the deviation occur as an immediate (step) decrease of the flow lasting for 10 min or more, or is it only an impulse? Is this decrease continuous at some rate? Answers to these questions may be obtained by an appropriate mathematical model (Švandová et al., 2005a; Švandová et al., 2005b; Labovský

et al., 2007a; Labovský et al., 2007b). In such a model approach, the extent of the deviations may be easily incorporated and possible consequences can be investigated. The basis of this methodology is the integration of mathematical modelling into the HAZOP study. This integration is useful for the identification of consequences of the generated deviations, and the suggestion of corrective actions. Moreover, the integration of mathematical modelling into the HAZOP study may potentially lead to the detection of some unexpected deviations. Other advantages of this approach are:

1. significantly reduced time and effort required in HAZOP;
2. more smooth and detailed HAZOP study;
3. minimisation of the influence of human factors.

3. Impact of mathematical model selection on the prediction of steady state and dynamic behaviour of a reactive distillation column

As a model system, the MTBE reaction system was chosen:

$$CH_3OH + (CH_3)_2\,C = CH_2 \Leftrightarrow (CH_3)_3\,COCH_3 \tag{18}$$

where iso-butene (IB) reacts with methanol (MeOH) to form MTBE in a reversible, exothermic reaction. The reaction is catalysed by a strong ion-exchange resin. The reaction rate equation and its parameters were given by Rehfinger and Hoffmann (1990). Possible side-reactions were ignored. Reaction rates were calculated assuming a pseudo-homogenous model. The reaction is usually carried out in the presence of inert components.

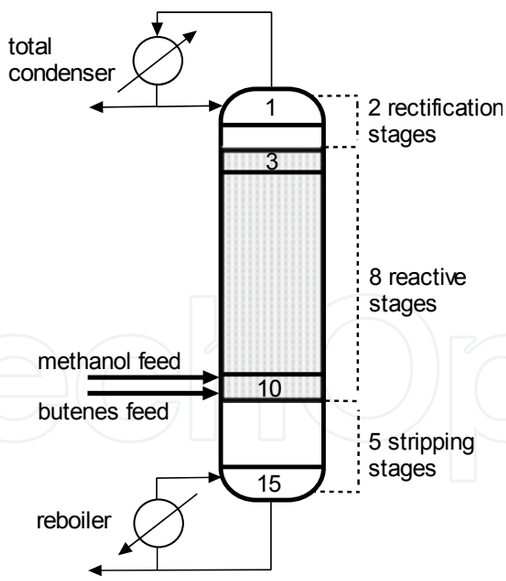

Fig. 3. Reactive distillation column

These inert components result from upstream processing, where isobutene is produced. In our case study, 1-butene was used as an inert. The vapour–liquid equilibrium was calculated using the UNIQUAC model with the binary interaction parameters reported by Rehfinger and Hoffmann (1990) (all binary interactions between MeOH, IB, MTBE) and HYSYS 2.1 (all binary interactions between 1-butene and the other components). The gas

phase was assumed to be ideal. Physico-chemical properties of all pure components were taken from the HYSYS 2.1 database. The column configuration chosen for the simulations is the one described by Jacobs and Krishna (1993) (see Fig. 3).The column consisted of a total condenser, 15 sieve trays (2 rectifying stages, 8 reactive stages and 5 stripping stages), and a partial reboiler. On each of the eight stages in the reactive zone, 1000 kg of the catalyst were charged in the form of "envelopes" placed along the flow path length. Details of such a construction are available in a patent (Jones Jr., 1985). The column pressure was 1110 kPa and the column had two feed streams: a methanol feed and a mixed butenes feed, both fed to stage 10. At a standard operating point, the molar flow rates of methanol and the mixture of butenes were 775.8 and 1900 kmol h^{-1}, respectively. The mixed butenes feed consisted of 35.58% isobutene and 64.42% 1-butene. The reflux ratio was set to 7 and the bottom flow rate to 675 kmol h^{-1}. Detailed specifications of the sieve trays are given in Table 5.

Tray specifications			*Tray specifications*		
Type of tray	Sieve	-	Number of liquid flow passes	5	-
Column diameter	6	m	Fractional active area	0.76	-
Total tray area	28.27	m^2	Fractional hole area	0.1	-
Tray spacing	0.61	m	Fractional downcomer area	0.12	-
Hole diameter	4.5	mm	Liquid flow path length	0.97	m
Weir height	50	mm	Total weir length	22	m

Table 5. Specifications of reactive distillation column tray

3.1 Equilibrium vs. nonequilibrium stage model

The objective of this part is to compare the prediction of the equilibrium and nonequilibrium models during the safety analysis of a reactive distillation column focusing on the identification of hazardous situations or operability problems. The safety and operability analyses are based on the application of the HAZOP procedure integrated with a mathematical model with the aim to determine the column response to deviations from normal operation conditions or during a nonstandard procedure, like the start-up of the reactive distillation column. Mathematical models used for this study were described in detail in the previous part of this chapter. In the EQ model, the stage efficiency of 60% was assumed. This value closely corresponded to the calculations of the NEQ model using the AICHE calculation method for sieve tray mass transfer (Baur et al., 2000). Identification of the multiple steady states locus in two parameter planes (remaining operation parameters were kept constant) was performed using the algorithm CONT (Kubíček, 1976; Marek & Schreiber, 1991). The result of these simulations is depicted in Fig. 4, where the methanol feed flow rate and the butenes feed flow rate were chosen as the parameters of interest. The bifurcation diagram contains information about the limit points and the multiplicity intervals. White area in this diagram indicates that for the combination of both investigated parameters only one steady state is possible, meanwhile, the filled area represents the three possible steady states for the actual methanol and butenes feed flow rates. The boundary lines of the filled area present the limit points in the investigated parametric plane.

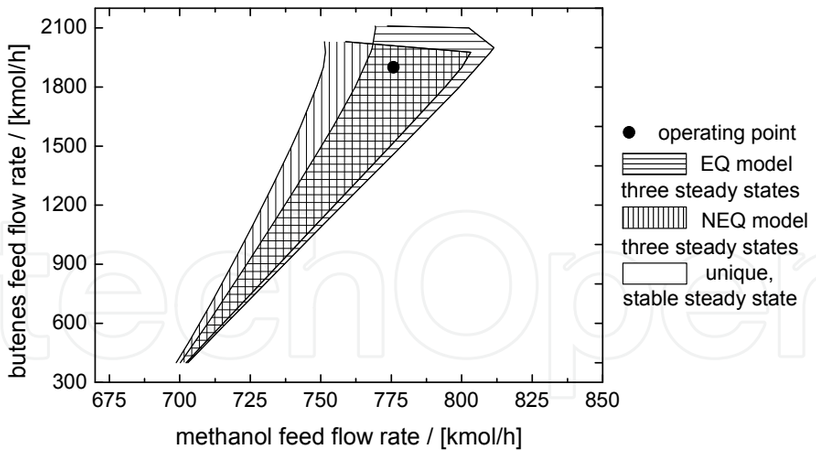

Fig. 4. Bifurcation diagram in the parametric plane methanol feed flow rate and butenes feed flow rate (reprinted from Švandová et al. (2009))

Fig. 4 indicates that the multiplicity zones predicted by EQ and NEQ models do not overlap in the whole range of the investigated parameters; however, for the operational methanol feed flow rate (775.8 kmol h^{-1}) and the operational butenes feed flow rate (1900 kmol h^{-1}), the steady-state multiplicity was predicted assuming both models (black circle in Fig. 4). Fig. 4 provides information about multiplicity intervals; however, it does not give information about conversion in the possible steady states. This information is provided by the solution diagrams (Figs. 5A and B). In the solution diagrams, either the methanol feed flow rate (with constant butenes feed flow rate set to the value of 1900 kmol h^{-1}) or the butenes feed flow rate (with constant methanol feed flow rate set to the value of 775.8 kmol h^{-1}) were considered as continuation parameters. The solution diagrams (Fig. 5A), where the methanol feed flow rate was used as a continuation parameter, indicate three steady states at the operating value of the methanol feed flow rate (775.8 kmol h^{-1}) for both models. These curves of the iso-butene conversion are continuous. The bifurcation diagram (Fig. 5B.), with the butenes feed flow rate used as a continuation parameter, indicates the same three steady states for both models used at the operational value of the butenes feed flow rate (1900 kmol h^{-1}) as those in Fig. 5A. However, very interesting results of these continuations are continuous curves of the iso-butene conversion with isolas located above these curves for both investigated models (Fig. 5B). From both solution diagrams (Figs. 5A and B) follows that the iso-butene conversion in the upper steady states are nearly identical for both used models. The conversion of iso-butene is relatively different in the lower steady state. Analysis of the methanol feed flow rate solution diagram (Fig. 5A) implies that a decrease in the methanol flow rate does not cause rapid decrease of the iso-butene conversion. A different situation occurs when the methanol flow rate is changed to a higher value. An increase in the methanol flow rate can lead to a rapid decrease of the iso-butene conversion. Similar situations can be expected for a rapid decrease or increase of the butenes feed flow rate. As it can be seen, solution diagrams obtained by the EQ and NEQ models are not identical in the whole range of the investigated parameters, what can results in different predictions of the reactive distillation column behaviour during dynamic simulations following the HAZOP procedure. As it was already mentioned, the HAZOP analysis is quite complex and time-consuming. Therefore, only one deviation is analysed and discussed in the text below.

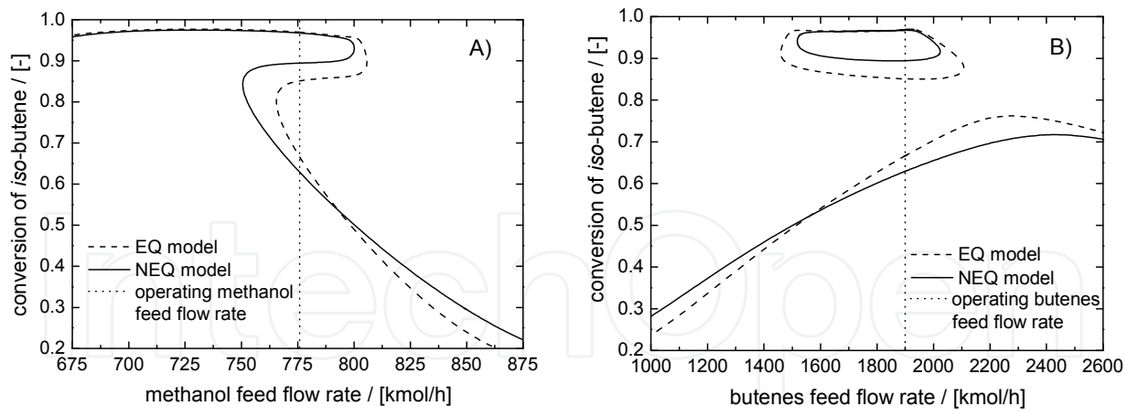

Fig. 5. Solution diagrams obtained by the EQ and NEQ models. Continuation parameter: A) methanol feed flow rate, B) butenes feed flow rate (reprinted from Švandová et al. (2009))

Let us summarise some very important information for this simple example of the HAZOP procedure:

Studied equipment: *reactive distillation column*
Chosen node for HAZOP analysis: *feed stream of butenes*
Investigated parameter: *feed flow rate of butenes*
Designed steady state operation value of this parameter: *1900 kmol h^{-1}*
Used guideword: *higher*
Created deviation: *higher butenes feed flow rate*

Fig. 6A–C shows consequences predicted by the EQ and NEQ models for the deviation "higher butenes feed flow rate". At the time of 1 h, the butenes feed flow rate suddenly increased from the operational value of 1900 to 1995 kmol h^{-1} (+5%; Fig. 6A), to the value of 2090 kmol h^{-1} (+10%; Fig. 6B) and finally to 2185 kmol h^{-1} (+15%; Fig. 6C). In all three cases, time duration of the deviation was 10 h and the reactive distillation column was forced to find a new steady state corresponding to the new value of the butenes feed flow rate. At the time of 11 h, the butenes feed flow rate returned back to the operational value (1900 kmol h^{-1}). Fig. 6A shows a situation when the butenes feed flow rate was changed by about 5%. Both, EQ and NEQ, models predicted that after the butenes flow rate returns to the operational value, the reactive distillation column will return to the original steady state characterised by high conversion of iso-butene. Different situation is depicted in Fig. 6B, the butenes feed flow rate was changed by about 10%. After returning the butenes flow rate to the operational value, the reactive distillation column stabilised in a lower stable steady state considering the NEQ model. However, when the EQ model was used to simulate the reactive distillation column, the conversion of iso-butene returned to the original steady state after the perturbation. These results indicate a notable disagreement in the prediction considering the EQ and the NEQ model. Fig. 6C shows the situation when the butenes feed flow rate was changed by about 15%. Both models predicted that after the butenes flow rate returns to the operating value, the reactive distillation column stabilises in a lower stable steady state. From Figs. 6A–C follows that the magnitude of the deviations has a significant influence on the deviation consequences; however, the consequences prediction can be different considering the EQ or the NEQ model (Fig. 6B). In many cases, duration of the failure may dramatically affect the response of the device although this aspect is not usually

investigated during a "typical" HAZOP procedure. Thus, for the next simulation, the same deviation, higher butenes feed flow rate, was taken into account.

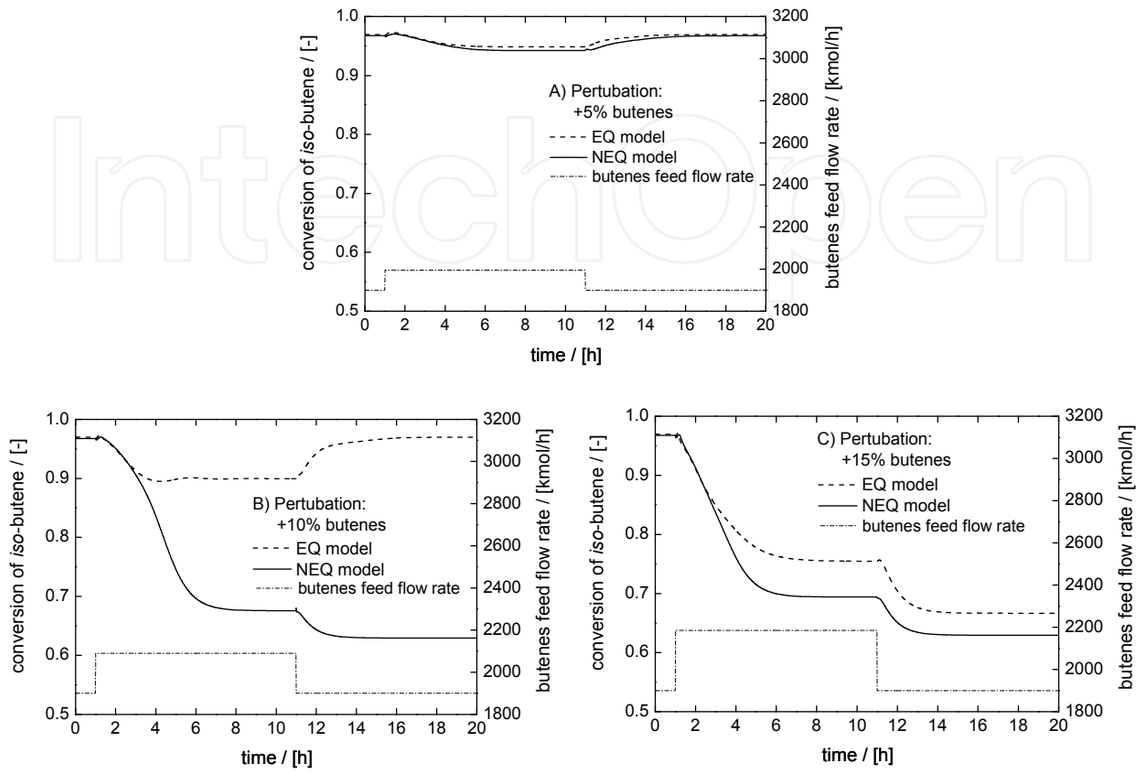

Fig. 6. Conversion changes predicted by the EQ and NEQ models caused by change of the butenes feed flow rate. Deviation extension: (A) +5%, (B) +10% and (C) +15% (reprinted from Švandová et al. (2009))

Fig. 7 presents dynamic simulations of an RD column, starting from the operating steady states characterised by high-conversion of iso-butene. At the time equal to 1 h, a 15% increase of the butenes feed flow rate was simulated (the same deviation as in Fig. 6C). Dynamic responses to the perturbation durations varying from 0.5 to 5 h were investigated using the EQ (Fig. 7A) and NEQ (Fig. 7B) models. A system described by the EQ model switches to the lower conversion steady state only after a perturbation longer than 3 h (Fig. 7A). However, a system described by the NEQ model switches to the lower steady state earlier, at the perturbation duration of 2 h and more (Fig. 7B). From Figs. 7A and B it is clear that the time durations of the feed flow rate disturbances have an extensive impact on the transitions between parallel steady states; however, the prediction of column behaviour is different assuming the EQ and the NEQ model. A more complex comparison of the predictions of the equilibrium and nonequilibrium models during a safety analysis of a reactive distillation column focusing on the identification of hazardous situations or operability problems is provided in the article by Švandová et al. (2009). From the presented analysis follows an important conclusion: the proportion and localisation of the zones of multiple steady states in the solution diagrams predicted by the EQ and NEQ models can be partly different. For this reason, the EQ and NEQ models show different response to the HAZOP deviation "higher butenes feed flow rate". Time duration of the feed flow rate

disturbances has an extensive impact on the transitions between parallel steady states predicted by the EQ and NEQ models. It was shown that a reliable prediction of the reactive distillation column behaviour is influenced by the complexity of the mathematical model used for its description. The EQ model is simpler, requiring a lower number of model parameters. On the other hand, the assumption of equilibrium between the vapour and liquid streams leaving the reactor can be difficult to meet, especially if some perturbations of the process parameters occur. The NEQ model takes the interphase mass and heat transfer resistances into account. On the other hand, it is important to point out that prediction of the column behaviour is strongly dependent on the quality of the NEQ model parameters depending on the equipment design; this topic will be analysed in the next section.

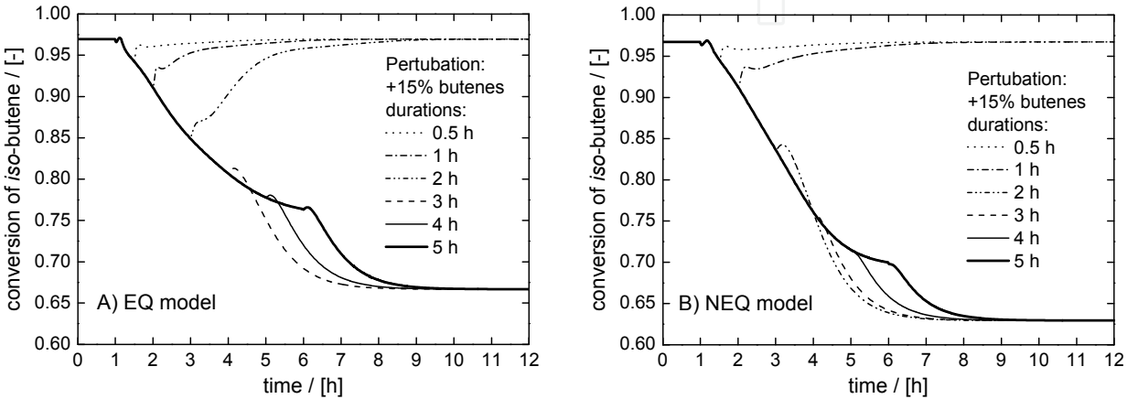

Fig. 7. Dynamic response obtained using (A) EQ model and (B) NEQ model to a 15% increase in the butenes feed flow rate 1 h after the simulation start. The perturbation period varied from 0.5 to 5 h (reprinted from Švandová et al. (2009))

3.2 Impact of mass transfer coefficient correlations on prediction of reactive distillation column behaviour

Model number	Mass transfer coefficient correlation	Style of line in graphs
1	AICHE (1958)	dashed line (■)
2	Chan-Fair (1984)	thick solid line (●)
3	Chen-Chuang (1993)	dash-dotted line (▲)
4	Zuiderweg (1982)	thin solid line (♦)

Table 6. Mass transfer coefficient correlations chosen for investigation

To compare the reactive distillation column behaviour predicted by different correlations for mass transfer coefficients, the four correlations summarised in Table 6 were chosen. The equations are available in the previous section (see Table 4). To estimate the diffusion coefficients in gas mixtures and in dilute liquid mixtures, empirical correlations of Fuller-Schettler-Giddings (1966) and Wilke-Chang (1955), respectively, were used (for details see Reid (1977), Taylor & Krishna (1993), Perry et. al. (1997)). The Maxwell-Stefan diffusion coefficient is defined for each binary pair in the multicomponent liquid mixture using the diffusion coefficients in dilute liquid. The mixing rule used was taken from Wesselingh and

Krishna (1990). In the solution diagrams (Figs. 8a and b), either the methanol feed flow rate or the butenes feed flow rate were the continuation parameters. The conversion of isobutene was examined. The solution diagrams (Fig. 8a), where the methanol feed flow rate was used as the continuation parameter, indicate that multiple steady states are predicted by Models 1 and 2. Using parameters calculated by Models 3 and 4, no multiplicity occurred in the whole range of the investigated parameters. When the isobutene feed flow rate was used as the continuation parameter, multiple steady states were found for three of the four investigated models (Fig. 8b).

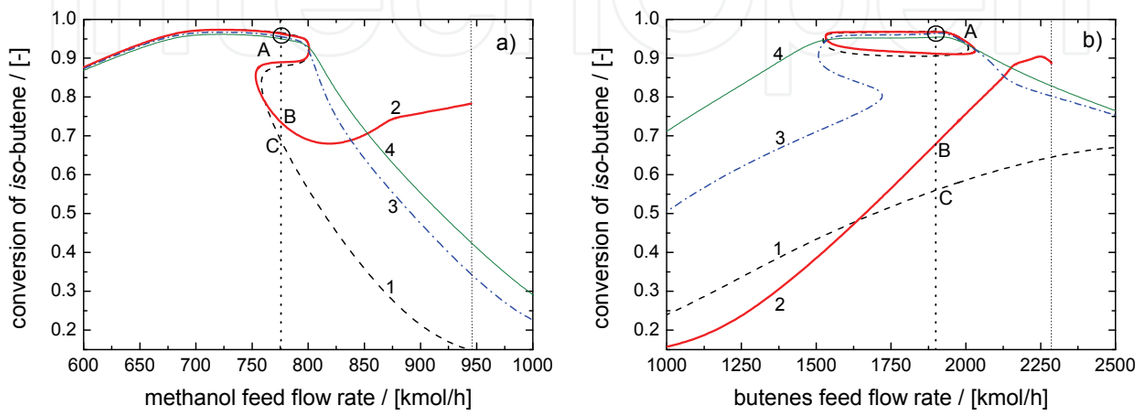

Fig. 8. a) Conversion of isobutene vs. methanol feed flow rate solution diagrams. b) Conversion of isobutene vs. butenes feed flow rate solution diagrams (dashed line—Model 1, thick solid line—Model 2, dash-dotted line—Model 3, thin solid line—Model 4, vertical dotted line—operating feed flow rate, vertical short dotted line—Model 2 out of the validity range) (reprinted from Švandová et al. (2008))

Only when using parameters calculated by Model 4, no multiplicity occurred in the whole range of the investigated parameters. However, a very interesting result is that Models 1 and 2 predict continuous curves of the isobutene conversion with isolas located above these curves. Model 3 predicts a typical 'S' profile of the isobutene conversion and, at the same time, the "window" in which these multiplicities occur is significantly reduced (see Fig. 8b). In general, the AICHE method (Model 1) and the Chan-Fair method (Model 2) behave in essentially the same way, except for the strong dependence on the fraction of flooding in the Chan- Fair method (Model 2). The critics of the Chan-Fair (Model 2) correlation mention that the quadratic dependence on the fractional approach to flooding limits this correlation to the range of fractions of flooding where the quadratic term is positive (the fraction of flooding must lie between 0 and 1.2) (Kooijman & Taylor, 1995). We have encountered situations of the Chan-Fair (Model 2) correlations providing negative mass transfer coefficient because the fraction of flooding was outside this range. It is clear that negative mass transfer coefficients are physically meaningless and at the same time, the program that implements our nonequilibrium model stopped converging to a solution. This situation is represented in the solution diagrams (Fig. 8) by a short vertical dotted line (methanol feed flow rate of ≈948 kmol h^{-1} in Fig. 8a. and butenes feed flow rate of ≈2280 kmol h^{-1} in Fig. 8b). From the solution diagrams (Figs. 8a and b) follows that for the given operating feed flow rate of methanol (775.8 kmol h^{-1}, see dotted line in Fig. 8a) and operating feed flow rate of butenes (1900 kmol h^{-1}, see dotted line in Fig. 8b) predict Models 1 and 2 three steady states (two

stable, one unstable); however, Models 3 and 4 predict only one steady state. The steady states obtained by Models 3 and 4 are nearly equal to the upper steady states given by Models 1 and 2. The presence of multiple steady states strongly influences the reactive distillation column behaviour during its start-up as well as during any disturbances of the input parameters. For illustration, disturbances of the butenes feed flow rate were studied (Fig. 9a) starting from the operational steady states characterised by high conversion of isobutene. At 1 h, a very fast increase of the butenes feed flow rate, over 2100 kmol h^{-1}, was simulated. The original flow rate of butenes was reached 10 h later. The duration of the disturbance was so long to show that for all investigated methods, a new steady state corresponding to the butenes feed flow rate of 2100 kmol h^{-1} was reached.

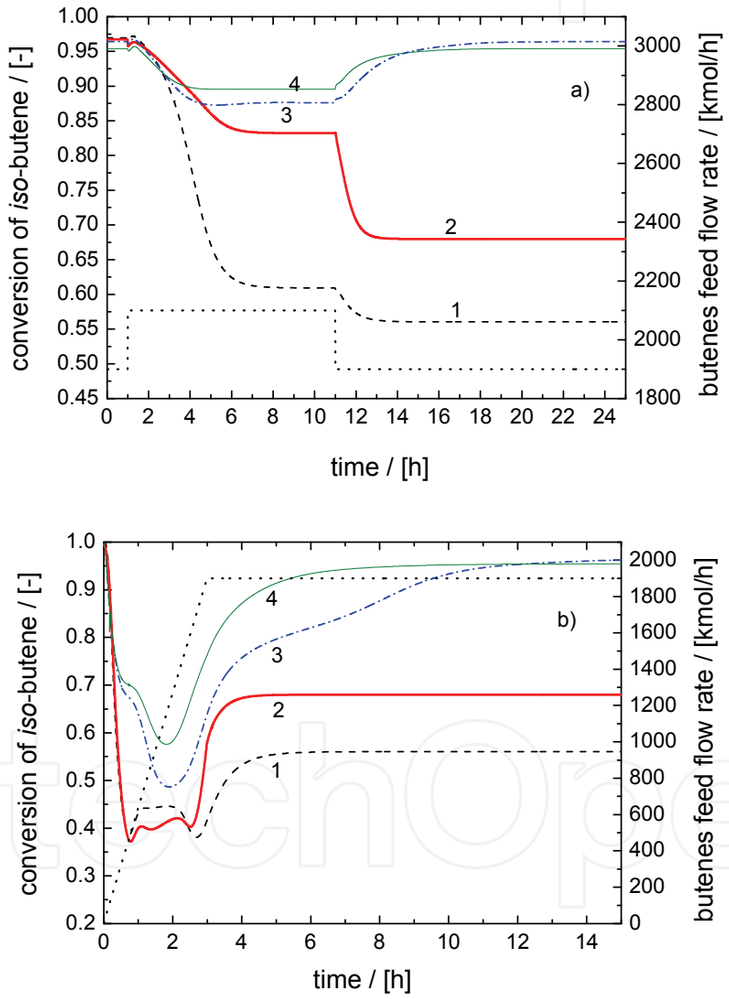

Fig. 9. a) Conversion of isobutene changes after step change of the butenes flow rate, b) Columns start-up considering a gradual increase of the butenes flow rate (dashed line—Model 1, thick solid line—Model 2, dash-dotted line—Model 3, thin solid line—Model 4, dotted line— butenes feed flow rate)

After returning the butenes flow rate to the operational value, the system described with the NEQ model using Models 1 and 2 was stabilised in the lower stable steady state. But

providing the NEQ model with Models 3 or 4, the system turned back to the original steady state (see Fig. 9a). From Fig. 9a follows that for situations predicted by Models 1 and 2, the restart of the RD column is needed to switch the conversion to higher steady states. Also, the presence of multiple steady states reduces the operability and controllability of the reactive distillation column during its start-up. This is confirmed by Fig. 9b which represents the column start-up considering a gradual increase of the butenes feed flow rate. Before the start-up procedure, the column was filled with pure methanol. Applying this start-up procedure, after reaching the operational feed flow rate of butenes, Models 1 and 2 predicted column stabilisation in the steady state characterised by low conversion of isobutene. Models 3 and 4 predict only one possible steady state for the operating feed flow rate of butenes (see Fig. 8b), hence, after the start-up procedure, this steady state is reached (Fig. 9b). From Fig. 8 follows that all used models predict the high conversion steady state in good agreement with each other.

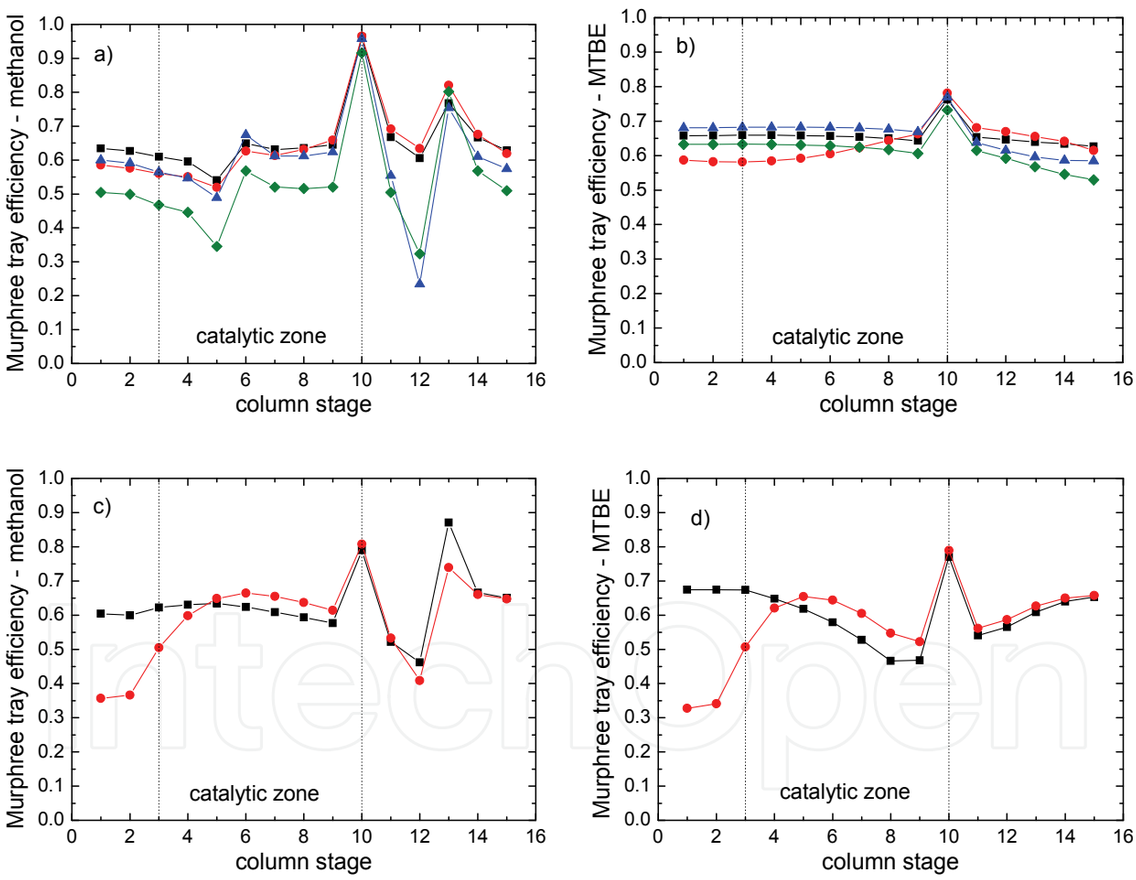

Fig. 10. a) Murphree tray efficiency in upper steady state for methanol, b) Murphree tray efficiency in upper steady state for MTBE, c) Murphree tray efficiency in lower steady state for methanol, d) Murphree tray efficiency in lower steady state for MTBE (■ - Model 1, ● - Model 2, ▲ - Model 3, ♦ - Model 4) (reprinted from Švandová et al. (2008))

This good tendency can be observed also in Figs. 10a-b which show the Murphree tray efficiency for methanol and MTBE, respectively, in the upper (high conversion) steady state.

These pictures indicate, that Model 4 tends to predict lower Murphree tray efficiency compared to other methods, however, this does not markedly affect the conversion of isobutene and the purity of MTBE in the reboiler. For the given operating conditions, the low conversion steady state was predicted only by Models 1 and 2. The difference between the low conversion steady states predicted by Models 1 and 2 is more relevant. Figs. 10c-d show the Murphree tray efficiency for methanol and MTBE, respectively, in the low conversion steady state. These pictures show that in the lower part of the reactive zone (stages 5-10) Model 2 predicts higher Murphree tray efficiency. Simultaneously, Model 2 predicts a radical decrease of the Murphree tray efficiency in the upper part of the column (stages 1-4). This behaviour predicted by Model 2 is caused by the quadratic dependence on the fractional approach to flooding, because in this part of the column is the fraction of flooding close to unity and thus close to flooding. As it was shown, different predictions of the reactive distillation column behaviour during dynamic change of the parameters depend on whether or not multiple steady state are expected for the required values of operational parameters. As it was already mentioned Models 1 and 2 predict multiple steady states for the operating value of butenes feed flow rate; however, Models 3 and 4 predict only one steady state. Fig. 11 shows isobutene conversion dependence on the butenes feed flow rate calculated using Model 1 (Fig. 11a) and Model 3 (Fig. 11b). In Fig. 11a, the AICHE method was used to calculate the mass transfer coefficients (solid line in Fig. 11a). Additional curves in Fig. 11a were calculated under the assumption that all mass transfer coefficients were higher (dashed line in Fig. 11a) or lower (dash-dotted line in Fig. 11a) by 10 %. Fig. 11b shows a similar investigation, however, to calculate the mass transfer coefficients, the Chen-Chuang method (solid line in Fig. 11b) was used. Dashed line and dash-dotted line in Fig. 11b were calculated with the assumption of a 10% increase and a 10 % decrease, respectively, of the mass transfer coefficients compared with those calculated using the Chen-Chuang method.

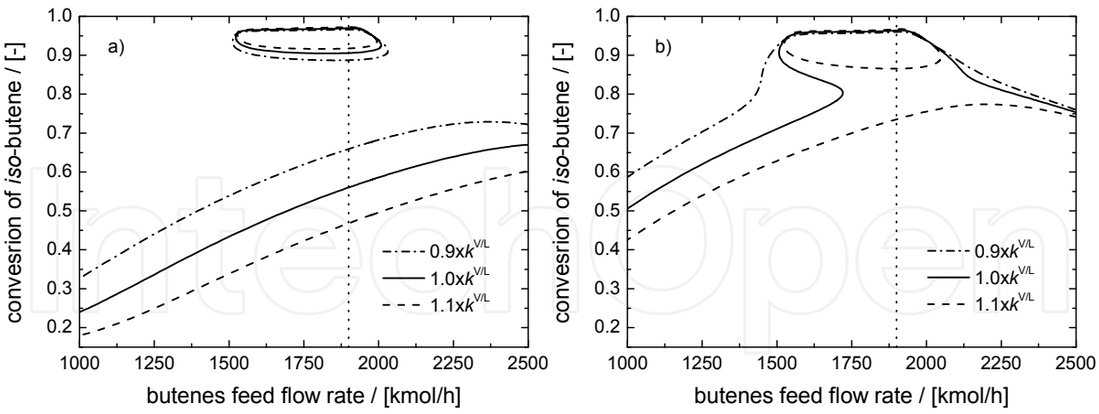

Fig. 11. Conversion of isobutene vs. butenes feed flow rate solution diagrams calculated using a) Model 1, b) Model 3 (solid lines – mass transfer coefficients predicted using correlations (Table 4), dash-dotted lines – mass transfer coefficients lower by 10%than coefficients predicted by correlations, dashed lines – mass transfer coefficient higher by 10% than coefficients predicted by correlations)

From Fig. 11a follows that a 10 % increase of the mass transfer coefficient value calculated using the AICHE method caused a decrease of the conversion in steady states located on the

lower branch and a decrease of the mass transfer coefficient caused an increase of the conversion in steady states located on the lower branch; however the number of steady states and quality of higher steady states located on isolas did not change. An interesting result is depicted in Fig. 11b. If the Chen-Chuang method is used to calculate the mass transfer coefficients, only one steady state is predicted for the operational feed flow rate of butenes (1900 kmol h^{-1}). Multiple steady states are predicted only for a short interval of butenes feed flow rate (approximately 1500- 1750 kmol h^{-1}). However, a 10 % increase of the mass transfer coefficients above the value calculated using the Chen- Chuang method (dashed line in Fig. 11b) caused that multiple steady states appeared for the operational feed flow rate of butenes and the shape of the calculated curves were significantly similar to those calculated using the AICHE method. On the other hand, a 10% decrease of the mass transfer coefficients below the value calculated using the Chen- Chuang method (dash-dotted line in Fig. 11a) caused that multiple steady states almost completely disappeared.

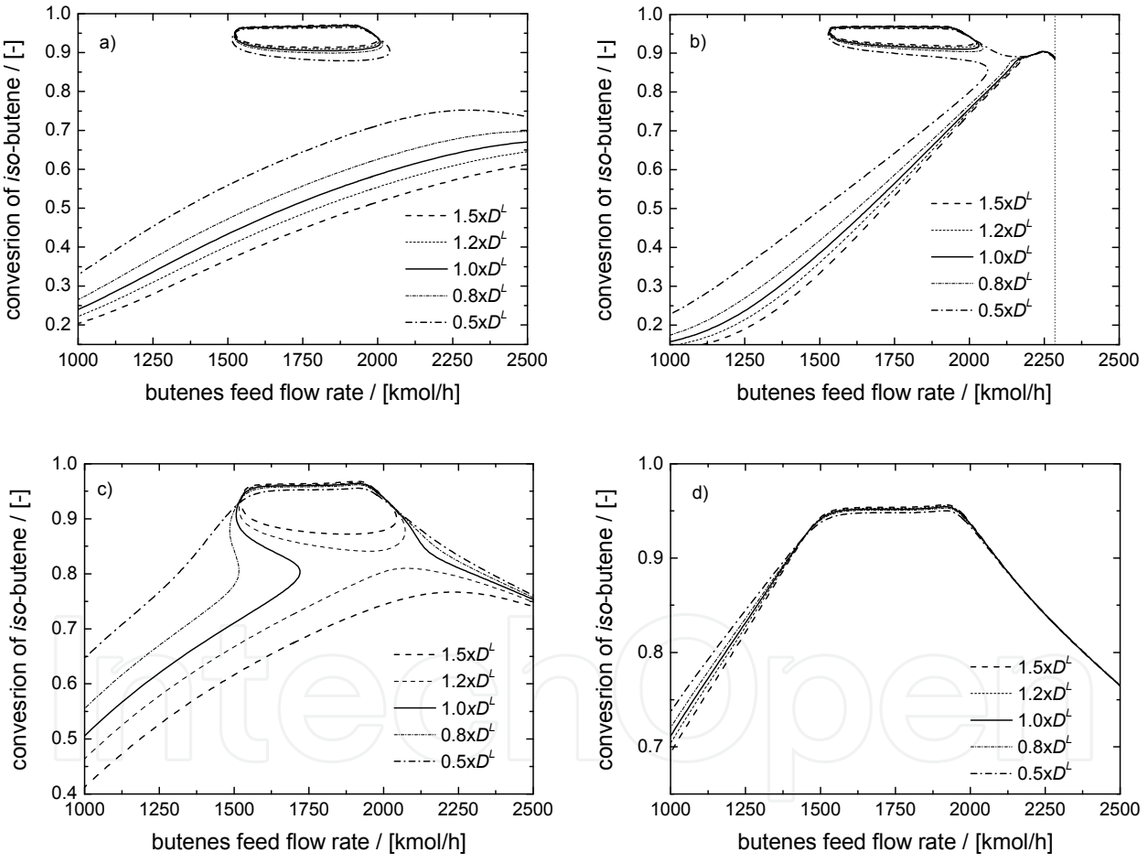

Fig. 12. Conversion of isobutene vs. butenes feed flow rate solution diagrams calculated using different liquid phase diffusion coefficient (±20%, ±50%) for all investigated models: a) Model 1, b) Model 2, c) Model 3 , d) Model 4

From this follows that a 10 % change of the value of mass transfer coefficients may even affect the number of the predicted steady states and consequently the whole prediction of the reactive distillation column behaviour during dynamic change of parameters. Investigations presented in Fig. 11 were made under the assumption that all binary mass

transfer coefficients (as well as the liquid in the gas phase) are by 10 % higher or lower than those calculated using empirical correlations (AICHE, Chen-Chuang). This is a very rough assumption which implies a potential uncertainty of the input parameters (diffusivity in the liquid or vapour phase, surface tension, viscosity, density, etc.) needed for the calculation of the mass transfer coefficients according to the correlations. It is important to note that each input parameter needed for the mass transfer coefficient calculation may influence the general NEQ model steady state prediction relatively significantly. Fig. 12 shows isobutene conversion dependence on the butenes feed flow rate calculated using a) Model 1, b) Model 2, c) Model 3 , d) Model 4, whereby several different values of the diffusion coefficients in the liquid phase were used in each model. To calculate the diffusion coefficients in a dilute liquid mixture, the Wilke-Chang (1955) correlation was used, which corresponds to the solid lines in Fig. 12a-d. To show the effect of of the diffusion coefficient uncertainty on the NEQ models steady state prediction, a 20 % and 50 % increase as well as decrease of the calculated diffusion coefficients was assumed. From Fig. 12 follows that the effect of the liquid phase diffusion coefficients on the steady states prediction using different models for mass transfer coefficient prediction is significantly different. The most distinguishable influence can be noticed using Model 3 (i.e., the Chen- Chuang method, see Fig. 12c) where the decrease of the diffusion coefficients led to notable reduction of the multiple steady state zone and the course of the curves was similar to that predicted by Method 4 (i.e., the Zuiderweg method, see Fig. 12d). On the other hand, the increase of the diffusion coefficients led to isola closure and creation of a multiplicity zone similar to that predicted by Method 1 (i.e., the AICHE method, see Fig. 12a) and Method 2 (i.e., the Chan-Fair method, see Fig. 12b). The effect of diffusion coefficients variation is very similar for Method 1 and Method 2 whereas the same equation was used for the number of transfer units in the liquid phase. Method 4 (i.e., the Zuiderweg method, see Fig. 12d) shows the smallest dependence on the diffusion coefficients change.

4. Conclusion

A reliable prediction of the reactive distillation column behaviour is influenced by the complexity of the mathematical model which is used for its description. For reactive distillation column modelling, equilibrium and nonequilibrium models are available in literature. The EQ model is simpler, requiring a lower number of the model parameters; on the other hand, the assumption of equilibrium between the vapour and liquid streams leaving the reactor can be difficult to meet, especially if some perturbations of the process parameters occur. The NEQ model takes the interphase mass and heat transfer resistances into account. Moreover, the quality of a nonequilibrium model differs in dependence of the description of the vapour–liquid equlibria, reaction equilibria and kinetics (homogenous, heterogeneous reaction, pseudo-homogenous approach), mass transfer (effective diffusivity method, Maxwell - Stefan approach) and hydrodynamics (completely mixed vapour and liquid, plug-flow vapour, eddy diffusion model for the liquid phase, etc.). It is obvious that different model approaches lead more or less to different predictions of the reactive distillation column behaviour. As it was shown, different correlations used for the prediction of the mass transfer coefficient estimation lead to significant differences in the prediction of the reactive distillation column behaviour. At the present time, considerable progress has been made regarding the reactive distillation column hardware aspects (tray

design and layout, packing type and size). If mathematical modelling is to be a useful tool for optimisation, design, scale-up and safety analysis of a reactive distillation column, the correlations applied in model parameter predictions have to be carefully chosen and employed for concrete column hardware. A problem could arise if, for a novel column hardware, such correlations are still not available in literature, e.g. the correlation and model quality progress are not equivalent to the hardware progress of the reactive distillation column.

As it is possible to see from Figs. 8a and b, for given operational conditions and a "good" initial guess of the calculated column variables (V and L concentrations and temperature profiles, etc.), the NEQ model given by a system of non-linear algebraic equations converged practically to the same steady state with high conversion of isobutene (point A in Fig. 8) with all assumed correlations. If a "wrong" initial guess was chosen, the NEQ model can provide different results according to the applied correlation: point A for Models 3 and 4 with high conversion of isobutene, point B for Model 2 and point C for Model 1. Therefore, the analysis of multiple steady-states existence has to be done as the first step of a safety analysis. If we assume the operational steady state of a column given by point A, and start to generate HAZOP deviations of operational parameters, by dynamic simulation, we can obtain different predictions of the column behaviour for each correlation, see Fig. 9a. Also, dynamic simulation of the column start-up procedure from the same initial conditions (for NEQ model equations) results in different steady states depending on chosen correlation, see Fig. 9b.

Our point of view is that of an engineer who has to do a safety analysis of a reactive distillation column using the mathematical model of such a device. Collecting literature information, he can discover that there are a lot of papers dealing with mathematical modelling. As was mentioned above, Taylor and Krishna (Taylor & Krishna, 2000) cite over one hundred papers dealing with mathematical modelling of RD of different complexicity. And there is a problem: which model is the best and how to obtain parameters for the chosen model. There are no general guidelines in literature. Using correlations suggested by authorities, an engineer can get into troubles. If different models predict different multiple steady states in a reactive distillation column for the same column configuration and the same operational conditions, they also predict different dynamic behaviour and provide different answers to the deviations generated by HAZOP. Consequently, it can lead to different definitions of the operator's strategy under normal and abnormal conditions and in training of operational staff.

5. Acknowledgement

This work was supported by the Slovak Research and Development Agency under the contract No. APVV-0355-07.

6. Nomenclature

A_b	bubbling area of a tray, m^2 (Table 4)
A_h	hole area of a sieve tray, m^2 (Table 4)
A	interfacial area per unit volume of froth, $m^2\ m^{-3}$ (Eqs. (15),(16))
a^I	net interfacial area, m^2

b	weir length per unit of bubbling area, m^{-1} (Table 4)
C_p	heat capacity, J mol^{-1} K^{-1}
c	molar concentration, mol m^{-3}
$\mathcal{E}$	energy transfer rate, J s^{-1}
D	Fick's diffusivity, m^2 s^{-1}
$\mathbb{D}$	Maxwell-Stefan diffusivity, m^2 s^{-1}
F	feed stream, mol s^{-1}
F_f	fractional approach to flooding (Table 4)
FP	flow parameter (Table 4)
F_s	superficial F factor, $kg^{0.5}$ $m^{-0.5}$ s^{-1}(Table 4)
H	molar enthalpy, J mol^{-1}
$\Delta_r H$	reaction enthalpy, J mol^{-1}
h	heat transfer coefficient, J s^{-1} m^{-2} K^{-1}
h_L	clear liquid height, m (Table 4)
h_w	exit weir height, m (Table 4)
J	molar diffusion flux relative to the molar average velocity, mol m^{-2} s^{-1}
K_i	vapour-liquid equilibrium constant for component i
$[k]$	matrix of multicomponent mass transfer coefficients, m s^{-1}
L	liquid flow rate, mol s^{-1}
Le	Lewis number ($\lambda\rho^{-1}C_p^{-1}D^{-1}$)
M	mass flow rates, kg s^{-1} (Table 4)
N	number of transfer units
N_F	number of feed streams
N_I	number of components
N_R	number of reactions
$\mathcal{N}$	transfer rate, mol s^{-1}
n	number of stages
P	pressure of the system, Pa
PF	Pointing correction
ΔP	pressure drop, Pa
p	hole pitch, m (Table 4)
Q	heating rate, J s^{-1}
Q^L	volumetric liquid flow rate, m^3 s^{-1}(Table 4)
Q^V	volumetric vapour flow rate, m^3 s^{-1}(Eq.(17))
$[R]$	matrix of mass transfer resistances, s m^{-1}
r	ratio of side stream flow to interstage flow
Sc^V	Schmidt number for the vapour phase (Table 4)
T	temperature, K
t	time, s
t	residence time, s (Table 4)

U	molar hold-up, mol
u_s	superficial vapour velocity, m s^{-1}
u_{sf}	superficial vapour velocity at flooding, m s^{-1}
V	vapour flow rate, mol s^{-1}
W	weir length, m (Table 4)
x	mole fraction in the liquid phase
y	mole fraction in the vapour phase
Z	the liquid flow path length, m (Table 4)
z^P	mole fraction for phase P

Greek letters

β	fractional free area (Table 4)
$[\Gamma]$	matrix of thermodynamic factors
ε	heat transfer rate factor
κ	binary mass transfer coefficient, m s^{-1}
λ	thermal conductivity, W m^{-1} K^{-1}
μ	viscosity of vapour and liquid phase, Pa s
ν	stoichiometric coefficient
$\dot{\xi}$	reaction rate, mol s^{-1}
ρ	vapour and liquid phase density, kg m^{-3} (Table 4)
σ	surface tension, N m^{-1}

Superscripts

o	initial conditions
I	referring to the interface
L	referring to the liquid phase
V	referring to the vapour phase

Subscripts

av	averaged value
f	feed stream index
i	component index
j	stage index
m	mixture property
r	reaction index
t	referring to the total mixture

7. References

AICHE (1958). *AICHE Bubble Tray Design Manual*, AIChE, New York

Baur, R., Higler, A. P., Taylor, R. & Krishna, R. (2000). Comparison of equilibrium stage and nonequilibrium stage models for reactive distillation, *Chemical Engineering Journal,* 76(*1*), 33-47; ISSN: 1385-8947.

Fuller, E. N., Schettler, P. D. & Gibbings, J. C. (1966). A new method for prediction of binary gas-phase diffusion coefficints, *Industrial & Enegineering Chemistry,* 58(*5*), 18-27; ISSN: 0888-5885.

Górak, A. (2006). Modelling reactive distillation. *Proceedings of 33rd International Conference of Slovak Society of Chemical Engineering*, ISBN:80-227-2409-2, Tatranské Matliare, Slovakia, May 2006, Slovak University of Technology, Bratislava, SK, in Publishing House of STU.

Chan, H. & Fair, J. R. (1984). Prediction of point efficiencies on sieve trays. 2. Multicomponent systems, *Industrial & Engineering Chemistry Process Design Development,* 23(*4*), 820-827; ISSN: 0196-4305.

Chen, G. X. & Chuang, K. T. (1993). Prediction of point efficiency for sieve trays in distillation, *Industrial & Engineering Chemistry Research,* 32, 701-708; ISSN: 0888-5885.

Jacobs, R. & Krishna, R. (1993). Multiple Solutions in Reactive Distillation for Methyl tert-Butyl Ether Synthesis, *Industrial & Engineering Chemistry Research,* 32(*8*), 1706-1709; ISSN: 0888-5885.

Jones Jr., E. M. (1985). Contact structure for use in catalytic distillation, US Patent 4536373.

Kletz, T. (1999). *HAZOP and HAZAN*, Institution of Chemical Engineers, ISBN: 978-0852954218

Kooijman, H. A. & Taylor, R. (1995). Modelling mass transfer in multicomponent distillation, *The Chemical Engineering Journal,* 57(*2*), 177-188; ISSN: 1385-8947.

Kooijman, H. A. & Taylor, R. (2000). *The ChemSep book*, Libri Books on Demand, ISBN: 3-8311-1068-9, Norderstedt

Kotora, M., Švandová, Z. & Markoš, J. (2009). A three-phase nonequilibrium model for catalytic distillation, *Chemical Papers,* 63(*2*), 197-204; ISSN: 0336-6352.

Krishna, R. & Wesselingh, J. A. (1997). The Maxwell-Stefan approach to mass transfer, *Chemical Engineering Science,* 52(*6*), 861-911; ISSN: 0009-2509.

Krishnamurthy, R. & Taylor, R. (1985a). A nonequilibrium stage model of multicomponent separation processes I-Model description and method of solution, *AIChE Journal,* 31(*3*), 449-456; ISSN:1547-5905

Krishnamurthy, R. & Taylor, R. (1985b). A nonequilibrium stage model of multicomponent separation processes II-Comparison with experiment, *AIChE Journal,* 31(*3*), 456-465; ISSN:1547-5905

Kubíček, M. (1976). Algorithm 502. Dependence of solution of nonlinear systems on a parameter [C5], *Transaction on Mathematical Software,* 2(*1*), 98-107; ISSN 0098-3500.

Labovský, J., Švandová, Z., Markoš, J. & Jelemenský (2007a). Mathematical model of a chemical reactor-Useful tool for its safety analysis and design, *Chemical Engineering Science,* 62, 4915- 4919; ISSN: 0009-2509.

Labovský, J., Švandová, Z., Markoš, J. & Jelemenský (2007b). Model-based HAZOP study of a real MTBE plant, *Journal of Loss Prevention in the Process Industries,* 20(*3*), 230-237; ISSN: 0950-4230

Marek, M. & Schreiber, I. (1991). *Chaotic Behaviour of Deterministic Dissipative Systems*, Academia Praha, ISBN: 80-200-0186-7, Praha

Mohl, K.-D., Kienle, A., Gilles, E.-D., Rapmund, P., Sundmacher, K. & Hoffmann, U. (1999). Steady-state multiplicities in reactive distillation columns for the production of fuel

ethers MTBE and TAME: theoretical analysis and experimental verification, *Chemical Engineering Science,* 54(*8*), 1029-1043; ISSN: 0009-2509.

Molnár, A., Markoš, J. & Jelemenský, L. (2005). Some considerations for safety analysis of chemical reactors, *Trans IChemE, Part A: Chemical Engineering Research and Design,* 83(*A2*), 167-176; ISSN: 0263-8762.

Noeres, C., Kenig, E. Y. & Gorak, A. (2003). Modelling of reactive separation processes: reactive absorption and reactive distillation, *Chemical Engineering and Processing,* 42(*3*), 157-178; ISSN: 0255-2701.

Perry, R. H., Green, D. W. & Maloney, J. O. (1997). *Perry's Chemical Engineers' Handbook*, McGraw-Hill, ISBN 0-07-049841-5, New York

Rehfinger, A. & Hoffmann, U. (1990). Kinetics of methyl tertiary butyl ether liquid phase synthesis catalyzed by ion exchange resin--I. Intrinsic rate expression in liquid phase activities, *Chemical Engineering Science,* 45(*6*), 1605-1617; ISSN: 0009-2509.

Reid, R. C., Prausnitz, J. M., Sherwood, T. K. (1977). *The Properties of Gases and Liquids*, McGraw-Hill, ISBN: 0-07-051790-8, New York

Sláva, J., Jelemenský, L. & Markos, J. (2009). Numerical algorithm for modeling of reactive separation column with fast chemical reaction, *Chemical Engineering Journal,* 150(*1*), 252-260; ISSN: 1385-8947.

Sláva, J., Svandová, Z. & Markos, J. (2008). Modelling of reactive separations including fast chemical reactions in CSTR, *Chemical Engineering Journal,* 139(*3*), 517-522; ISSN: 1385-8947.

Sundmacher, K. & Kienle, A. (2002). *Reactive Distillation, Status a Future Directions*, Wiley-VCH Verlag GmbH & Co. KGaA, ISBN: 3-527-60052-3, Weinheim

Švandová, Z., Jelemenský, Markoš, J. & Molnár, A. (2005b). Steady state analysis and dynamical simulation as a complement in the HAZOP study of chemical reactors, *Trans IChemE, Part B: Process Safety and Environmental Protection,* 83(*B5*), 463 - 471; ISSN: 0957-5820.

Švandová, Z., Labovský, J., Markoš, J. & Jelemenský, Ľ. (2009). Impact of mathematical model selection on prediction of steady state and dynamic behaviour of a reactive distillation column, *Computers & Chemical Engineering,* 33, 788-793; ISSN: 0098-1354.

Švandová, Z., Markoš, J. & Jelemenský (2005a). HAZOP analysis of CSTR with utilization of mathematical modeling, *Chemical Papers,* 59(*6b*), 464-468; ISSN: 0336-6352.

Švandová, Z., Markoš, J. & Jelemenský, Ľ. (2008). Impact of mass transfer coefficient correlations on prediction of reactive distillation column behaviour, *Chemical Engineering Journal,* 140(*1-3*), 381-390; ISSN: 1385-8947.

Taylor, R., Kooijman, H. A. & Hung, J.-S. (1994). A second generation nonequilibrium model for computer simulation of multicomponent separation processes, *Computers & Chemical Engineering,* 18(*3*), 205-217; ISSN: 0098-1354.

Taylor, R. & Krishna, R. (1993). *Multicomponent Mass Transfer*, John Wiley & Sons, Inc., ISBN: 0-471-57417-1, New York

Taylor, R. & Krishna, R. (2000). Modelling reactive distillation, *Chemical Engineering Science,* 55(*22*), 5183-5229; ISSN: 0009-2509.

Wesselingh, J. A., Krishna, R. (1990). *Mass Transfer*, Ellis Horwood Ltd, ISBN:978-0135530252, Chichester, England

Wilke, C. R. & Chang, P. (1955). Correlations of Diffusion Coefficients in Dilute Solutions, *AiChE Journal,* 1(*2*), 264-270; ISSN:1547-5905

Zuiderweg, F. J. (1982). Sieve trays : A view on the state of the art, *Chemical Engineering Science,* 37(*10*), 1441-1464; ISSN: 0009-2509.

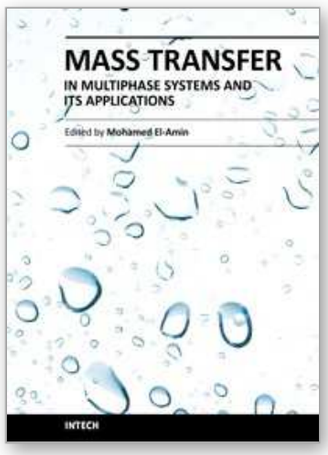

Mass Transfer in Multiphase Systems and its Applications
Edited by Prof. Mohamed El-Amin

ISBN 978-953-307-215-9
Hard cover, 780 pages
Publisher InTech
Published online 11, February, 2011
Published in print edition February, 2011

This book covers a number of developing topics in mass transfer processes in multiphase systems for a variety of applications. The book effectively blends theoretical, numerical, modeling and experimental aspects of mass transfer in multiphase systems that are usually encountered in many research areas such as chemical, reactor, environmental and petroleum engineering. From biological and chemical reactors to paper and wood industry and all the way to thin film, the 31 chapters of this book serve as an important reference for any researcher or engineer working in the field of mass transfer and related topics.

How to reference
In order to correctly reference this scholarly work, feel free to copy and paste the following:

Zuzana Švandová, Jozef Markoš and Ľudovít Jelemenský (2011). Impact of Mass Transfer on Modelling and Simulation of Reactive Distillation Columns, Mass Transfer in Multiphase Systems and its Applications, Prof. Mohamed El-Amin (Ed.), ISBN: 978-953-307-215-9, InTech, Available from: http://www.intechopen.com/books/mass-transfer-in-multiphase-systems-and-its-applications/impact-of-mass-transfer-on-modelling-and-simulation-of-reactive-distillation-columns

INTECH
open science | open minds

InTech Europe
University Campus STeP Ri
Slavka Krautzeka 83/A
51000 Rijeka, Croatia
Phone: +385 (51) 770 447
Fax: +385 (51) 686 166
www.intechopen.com

InTech China
Unit 405, Office Block, Hotel Equatorial Shanghai
No.65, Yan An Road (West), Shanghai, 200040, China
中国上海市延安西路65号上海国际贵都大饭店办公楼405单元
Phone: +86-21-62489820
Fax: +86-21-62489821

IntechOpen